Supporting Information for

Methane-Perylene Diimides-Based Small Molecule Acceptors for High Efficiency Non-Fullerene Organic Solar Cells

Gang Li *[a‡], Wenbin Yang [a‡], Shuaihua Wang [a‡] Tao Liu [ab‡]*, Cenqi Yan,[c] Gang Li,[c] Yu Zhang [a], Dandan Li [a], Xinyu Wang [a], Pin Hao [a], Jiewei Li, [d] Lijun Huo,[*e] He Yan[b]* and Bo Tang[a*]

[a] College of Chemistry, Chemical Engineering and Materials Science, Key Laboratory of Molecular and Nano Probes, Ministry of Education, Collaborative Innovation Center of Functionalized Probes for Chemical Imaging in Universities of Shandong, Institute of Materials and Clean Energy, Shandong Provincial Key Laboratory of Clean Production of Fine Chemicals, Shandong Normal University, Jinan 250014, P. R. China.

[b] Department of Chemistry and Energy Institute, The Hong Kong University of Science and Technology, Clear Water Bay, Hong Kong.

[c] Department of Electronic and Information Engineering, The Hong Kong Polytechnic University, Hong Hum, Kowloon, Hong Kong, China.

[d] Key Laboratory of Flexible Electronics (KLOFE) & Institute of Advanced Materials (IAM), Jiangsu National Synergetic Innovation Center for Advanced Materials (SICAM); Nanjing Tech University (NanjingTech), 30 South Puzhu Road, Nanjing, 211816, P.R. China.

[e] School of Chemistry, Beihang University, Beijing 100191, P. R. China

[‡]These authors contributed equally to this work.

Corresponding E-mail: ligang@sdnu.edu.cn; Liutaozhx@ust.hk; hyan@ust.hk; tangb@sdnu.edu.cn; huolijun@buaa.edu.cn

1. General information

All solvents and chemicals used were purchased from Energy Chemical and used without further purification. PDBT-T1[1] (Figure S4), compound bis(4'-(3,3,4,4-tetramethyl-2,5,1-dioxaboryl)phenyl)methane (1),[2] Tetrakis(4-(4,4,5,5-tetramethyl-1,3,2-dioxaborolan-2-yl)phenyl)methane (3), [3] PDI-Br (4)[4] were synthesized according to the reported literatures with minor modifications. TLC analyses were carried out by using Sorbent Technologies silica gel (200 mm) sheets. Column chromatography was performed on Sorbent silica gel 60 (40–63 mm). Solution NMR spectra were taken on a Bruker 400 MHz spectrometer in $CDCl_3$ at room temperature, both ^{1}H and ^{13}C NMR spectra were referenced to solvent residue peaks and the spectroscopic solvents were purchased from Cambridge Isotope Laboratories. Mass spectra were measured on a Bruker Maxis UHR-TOF MS spectrometer. UV−vis absorption spectra were performed with a Beijing Purkinje General Instrument Co. Ltd. TU-1901 spectrophotometer. All steady-state measurements were carried out using a quartz cuvette with a path length of 1 cm. Thermogravimetric analysis (TGA) was carried out on a TA Instrument TA Q50 Thermogravimetric Analyzer at a heating rate of 10 ^{o}C /min up to 600 ^{o}C.

2. Solar cell fabrication and characterization

Solar cells were fabricated in a conventional device configuration of ITO/PEDOT: PSS/active layer/ZrAcAc/Al. The ITO substrates were first scrubbed by detergent and then sonicated with deionized water, acetone and isopropanol subsequently, and dried overnight in an oven. The glass substrates were treated by UV-Ozone for 30 min before use. PEDOT: PSS (Heraeus Clevios P VP A 4083) layer was spin-cast onto the ITO substrates at 4000 rmp for 40s, and then dried at 150 ℃ for 15 min in air. The donor:acceptor blends with 1:1 ratio were dissolved in dichlorobenzene (the concentration of blend solutions are 20 mg/mL for all blend films), and stirred overnight in a nitrogen-filled glove box. The blend solution was spin-cast at 1600 rmp for 40s on the top of PEDOT: PSS layer followed by annealed at 100 ℃ for 5 min to remove the residual solvent. A thin ZrAcAc layer (10 nm) and Al layer (100 nm) were sequentially evaporated through a shadow mask under vacuum of 5×10^{-5} Pa. The area

of each device was 5.90 mm^2 defined by a shadow mask. The optimal blend thickness was about 95 nm, measured on a Bruker Dektak XT stylus profilometer. Current density-voltage (J-V) curves were measured in a Keithley 2400 Source Measure Unit. Photocurrent was measured in an Air Mass 1.5 Global (AM 1.5 G) solar simulator (Class AAA solar simulator, Model 94063A, Oriel) with an irradiation intensity of 100 mW cm^{-2}, which was measured by a calibrated silicon solar cell and a readout meter (Model 91150V, Newport). IPCE spectra were measured by using a QEX10 Solar Cell IPCE measurement system (PV measurements, Inc.).

3. Space charge-limited current (SCLC) device fabrication

The structure of electron-only devices is ITO/ZnO/active layer/ZrAcAc/Al and the structure of hole-only devices is ITO/MoO_X/active layers/MoO_X/Al. The fabrication conditions of the active layer films are same with those for the solar cells. The charge mobilities are generally described by the Mott-Gurney equation:

$$J = \frac{9}{8}\varepsilon_\gamma \varepsilon_0 \mu \frac{V^2}{L^3}$$

where *J* is the current density, ε_0 is the permittivity of free space (8.85×10^{-14} F/cm), ε_γ is the dielectric constant of used materials, μ is the charge mobility, *V* is the applied voltage and L is the active layer thickness. The ε_γ parameter is assumed to be 3, which is a typical value for organic materials. In organic materials, charge mobility is usually field dependent and can be described by the disorder formalism, typically varying with electric field, E=V/L, according to the equation:

$$\mu=\mu_0 exp[0.89\gamma\sqrt{\frac{V}{L}}]$$

Where μ_0 is the charge mobility at zero electric field and γ is a constant. Then, the Mott-Gurney equation can be described by:

$$J = \frac{9}{8}\varepsilon_\gamma \varepsilon_0 \mu_0 \frac{V^2}{L^3} exp[0.89\gamma\sqrt{\frac{V}{L}}]$$

4. Film and Device Characterization

The ultraviolet-visible (UV-Vis) absorption spectra of neat and blend films were obtained using a Shimadzu UV-3101 PC spectrometer. The current-voltage (*I-V*)

curves of all OSCs were measured in a high-purity nitrogen-filled glove box using a Keithley 2400 source meter. AM 1.5G irradiation at 100 mW/cm^2 provided by An XES-40S2 (SAN-EI Electric Co., Ltd.) solar simulator (AAA grade, 70×70 mm^2 photobeam size), which was calibrated by standard silicon solar cells (purchased from Zolix INSTRUMENTS CO. LTD). The external quantum efficiency (EQE) spectra of solar cells were measured in air conditions by a Zolix Solar Cell Scan 100. The morphology of the active layers was investigated by atomic force microscopy (AFM) using a Dimension Icon AFM (Bruker) in a tapping mode.

5. Electrochemical Characterization

Electrochemical measurements were performed under nitrogen in deoxygenated 0.1 M solutions of tetra-n-butylammonium hexafluorophosphate in dry dichloromethane using a CHI 660C electrochemical workstation, a glassy carbon working electrode, a platinum wire auxiliary electrode, and an Ag/AgCl reference electrode. Cyclic voltammograms were recorded at a scan rate of 50 mV s^{-1}. The lowest unoccupied molecular orbital (LUMO) levels were estimated based on the onset reduction potential (E_{red}), and the reduction potential was calibrated using ferrocene ($E_{Fc/Fc+}$) as a reference ($E_{red} = -[E_{measured} - E_{Fc/Fc+} + 4.8]$ eV). Ferrocene as an internal standard. Under the same condition, the onset oxidation potential of ferrocene was measured to be 0.336 V versus Ag/Ag$^+$.

6. AFM Characterization.

AFM measurements were performed by using a Scanning Probe Microscope-Dimension 3100 in tapping mode. All films were coated on ITO glass substrates.

7. Computational Studies

The geometry was optimized by density functional theory (DFT) using the B3LYP hybrid functional with basis set 6-31G(d).[5] Quantum chemical calculation was performed with the Gaussian 09 package. The long alkyl chains were replaced with an isopropyl group for simplification.

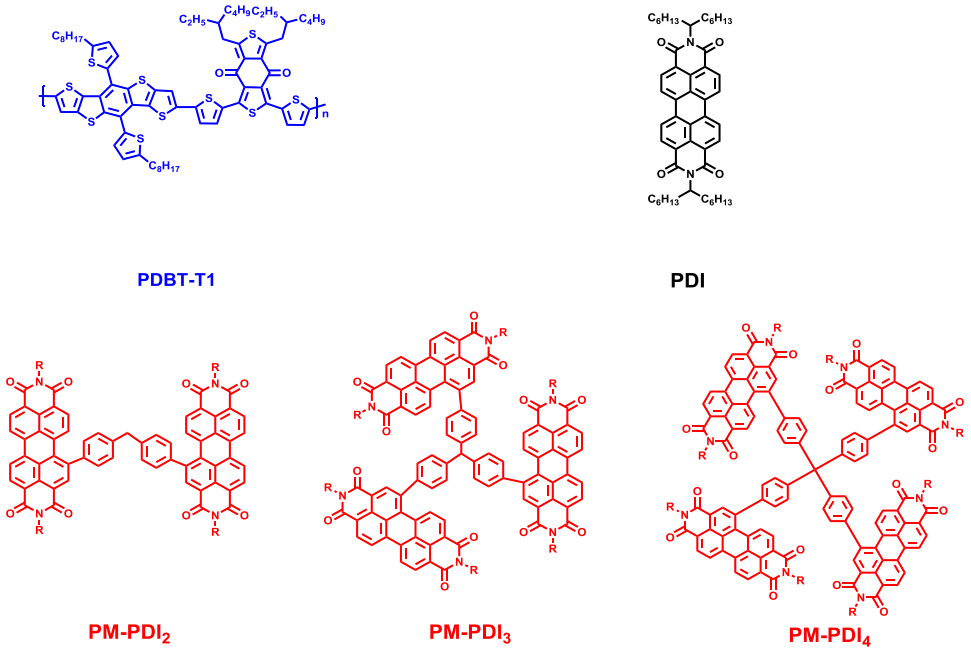

Figure S1. Molecular structures of **PDBT-T1**, **PM-PDI$_2$**, **PM-PDI$_3$** and **PM-PDI$_4$**.

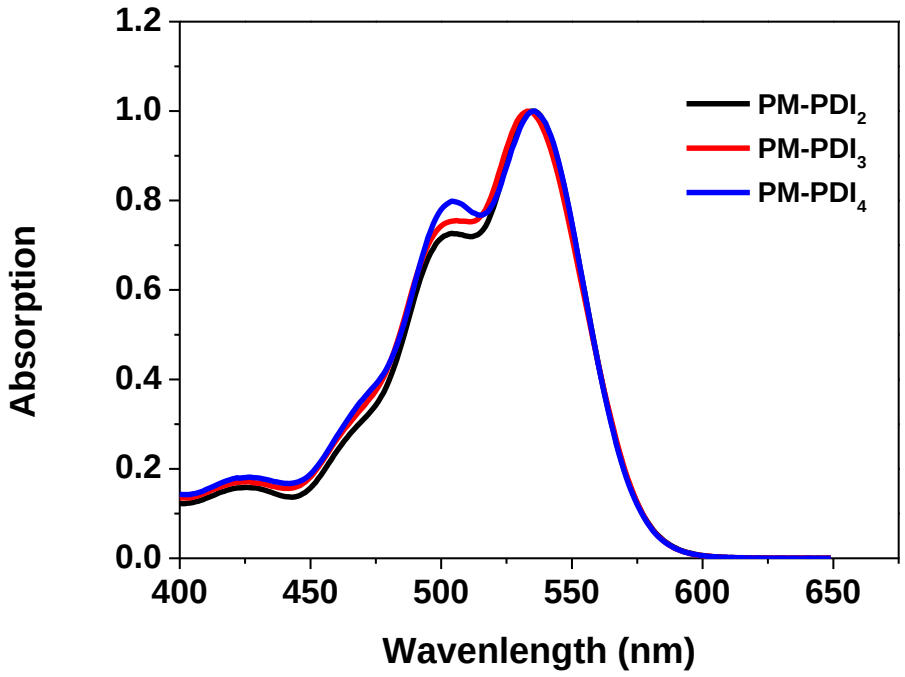

Figure S2. Absorption spectra of **PM-PDI$_2$**, **PM-PDI$_3$** and **PM-PDI$_4$** in dichloromethane solutions.

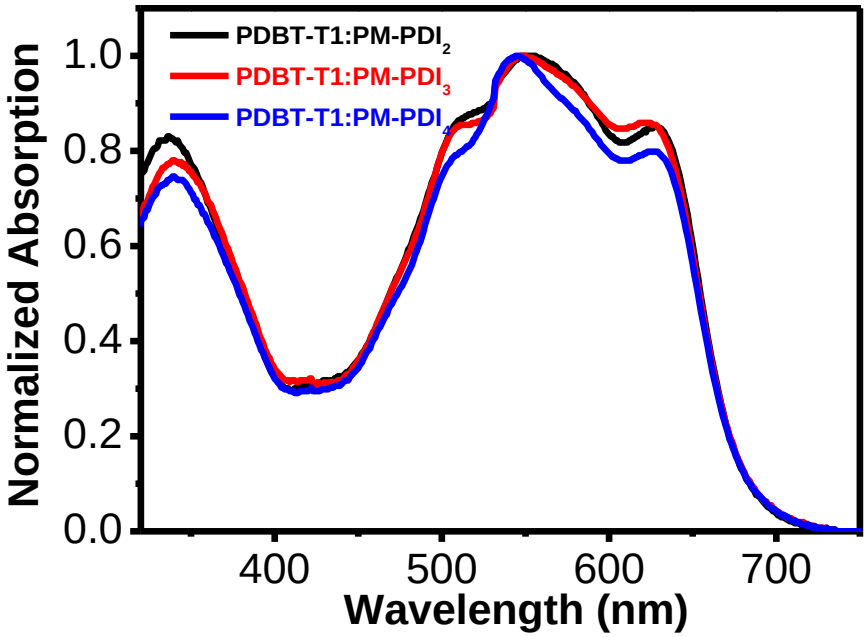

Figure S3. Absorption spectra of **PBDB-T1**, **PM-PDI$_2$**, **PM-PDI$_3$** and **PM-PDI$_4$** films.

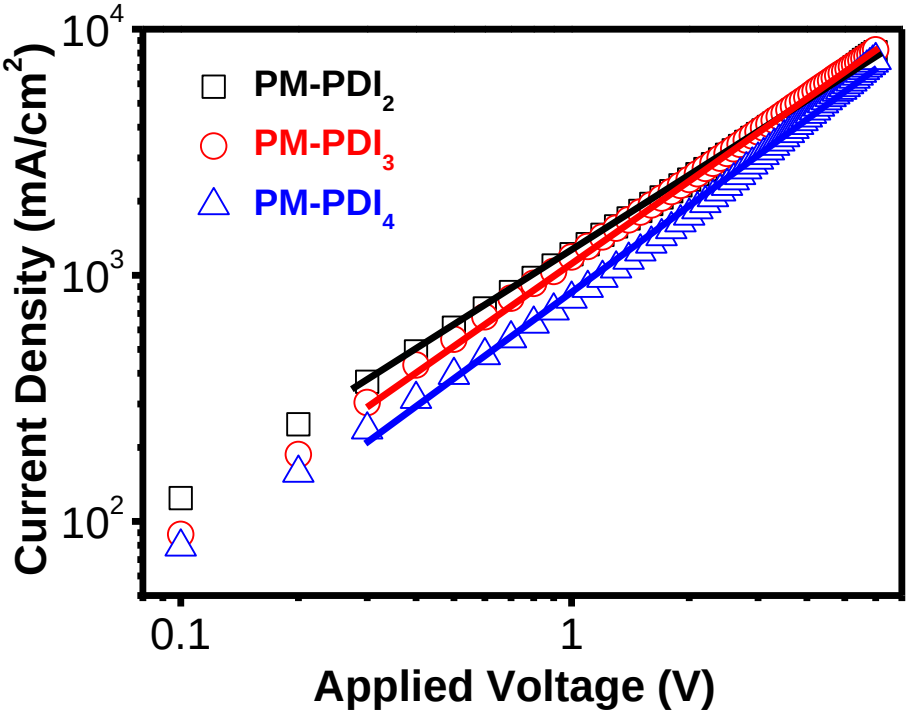

Figure S4. Dark current density-voltage characteristics for electron-only devices with optimized **PM-PDI$_2$**, **PM-PDI$_3$** and **PM-PDI$_4$** films.

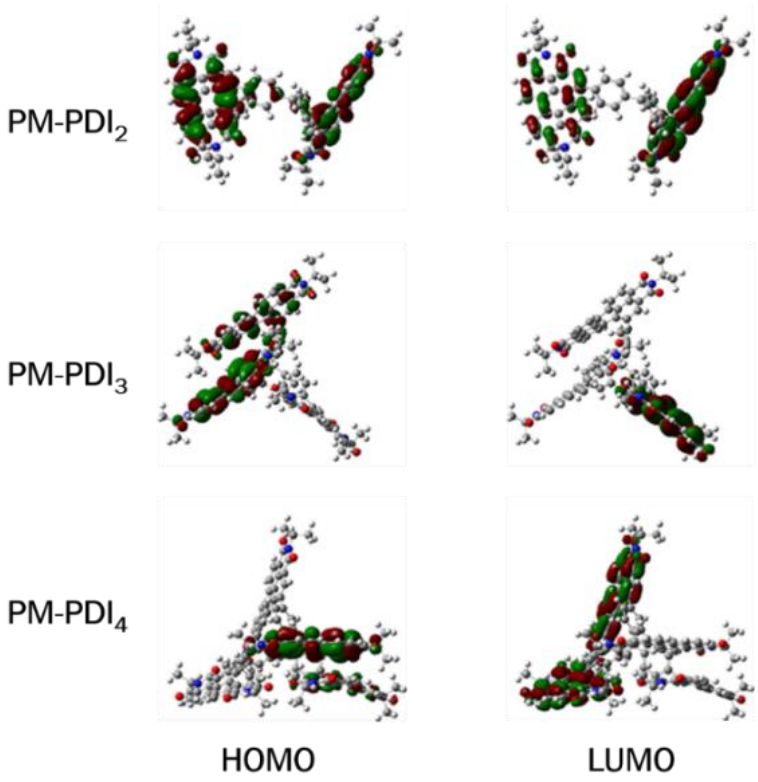

Figure S5. Optimized molecular geometries of **PM-PDI$_2$**, **PM-PDI$_3$** and **PM-PDI$_4$** at B3LYP/6-31G(d).

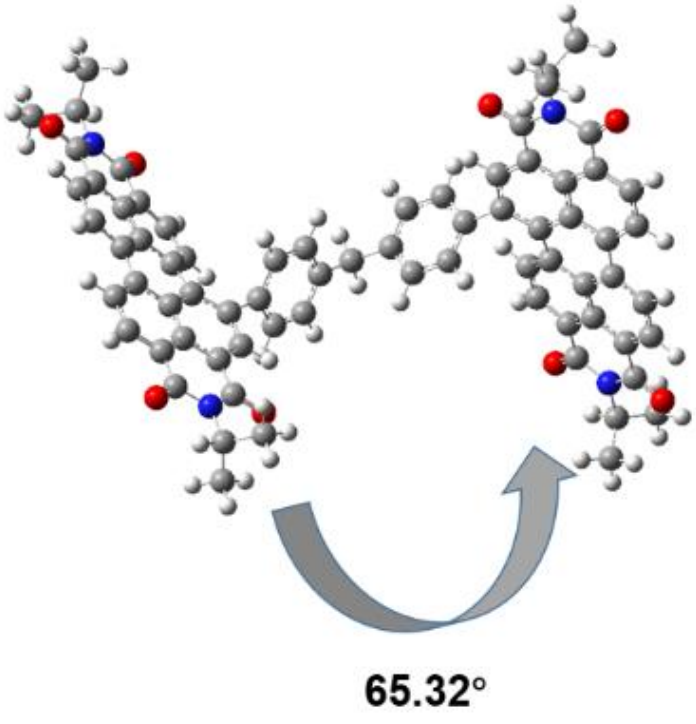

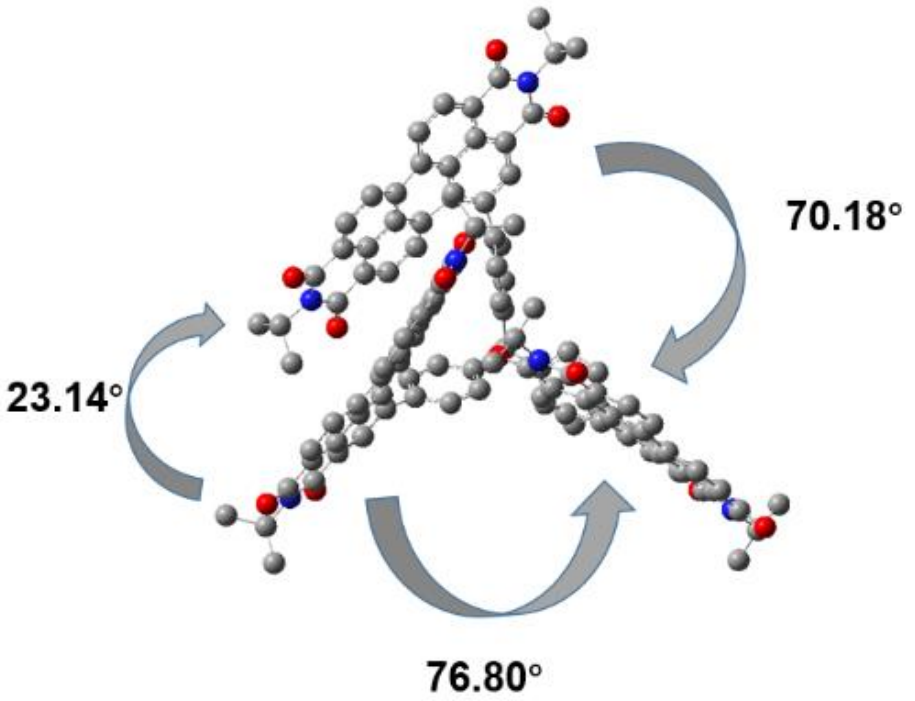

PM-PDI$_3$

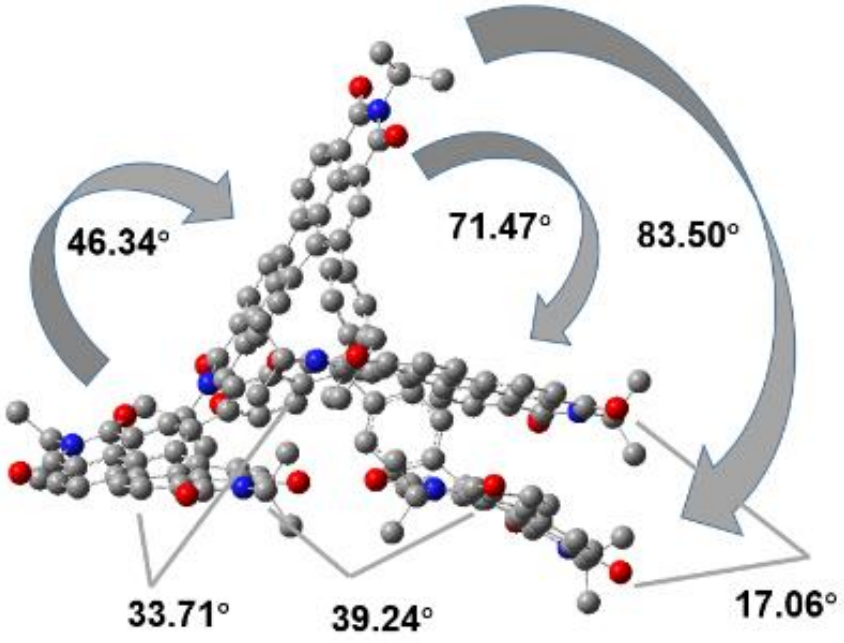

PM-PDI$_4$

Figure S6. Optimized molecular geometries of **PM-PDI$_2$**, **PM-PDI$_3$** and **PM-PDI$_4$** at B3LYP/6-31G(d).

Table S1. The calculated data of **PM-PDI$_2$**, **PM-PDI$_3$** and **PM-PDI$_4$**.

Samples	HOMO	LUMO	E_g
PM-PDI$_2$	-5.84	-3.38	2.46
PM-PDI$_3$	-5.74	-3.45	2.29
PM-PDI$_4$	-5.78	-3.43	2.35

Table S2. Hole and electron mobility of as-synthesized acceptors and blend films.

Samples	Hole mobility ($cm^2 V^{-1} s^{-1}$)	electron mobility ($cm^2 V^{-1} s^{-1}$)
PDBT-T1: PM-PDI$_2$	6.59×10^{-4}	3.01×10^{-4}
PDBT-T1: PM-PDI$_3$	7.54×10^{-4}	4.43×10^{-4}
PDBT-T1: PM-PDI$_4$	7.92×10^{-4}	4.53×10^{-4}
PM-PDI$_2$	-	5.78×10^{-4}
PM-PDI$_3$	-	7.08×10^{-4}
PM-PDI$_4$	-	7.39×10^{-4}

Table S3. Key photovoltaic parameters calculated from the J_{ph}-V_{eff} curves of **PDBT-T1: PM-PDI$_2$**, **PDBT-T1: PM-PDI$_3$** and **PDBT-T1: PM-PDI$_4$** based devices after annealing.

Samples	J_{sat}[a] (mA.cm^{-2})	J_{ph}[b] (mA.cm^{-2})	J_{ph}[c] (mA.cm^{-2})	J_{ph}[b]/ J_{sat} (%)	J_{ph}[c]/ J_{sat} (%)
PDBT-T1: PM-PDI$_2$	11.378	8.490	4.452	74.6	39.4
PDBT-T1: PM-PDI$_3$	11.875	11.022	9.223	92.8	77.6
PDBT-T1: PM-PDI$_4$	12.339	11.203	9.160	90.8	74.2

[a]The J_{ph} under condition of V_{eff} = 3.0 V; [b]The J_{ph} under short circuit condition; [c]The J_{ph} under maximum power output condition.

Table S4. Cost evaluation for the synthesis of **PM-PDI$_3$** (1 g).

	Commercial available chemicals	Price	Dosage	Cost
Step 1	p-dibromobenzene	25 g/55 RMB	2.41 g	5.30 RMB
	n-BuLi	100 mL/84 RMB	3.7 mL	3.11 RMB
	THF	500 mL/18 RMB	50 mL	1.8 RMB
	EtOAc	500 mL/8.8 RMB	250mL	4.4 RMB
	Na_2SO_4	500 g/10 RMB	2 g	0.04 RMB
	petroleum ether	500 mL/7.3 RMB	800 mL	11.68 RMB
	silica gel	500 g/15 RMB	200 g	6 RMB
	diethyl carbonate	100 mL/55 RMB	0.3 mL	0.17 RMB
Step 2	tris(4-bromophenyl)methanol		1.34 g	
	Formic acid	100 g/55 RMB	26 mL	17.45 RMB
	Na_2CO_3	500 g/20 RMB	30 g	1.2 RMB
	CH_2Cl_2	500 mL/8.8 RMB	120 mL	2.12 RMB
	Na_2SO_4	500 g/10 RMB	2 g	0.04 RMB
	silica gel	500 g/15 RMB	200 g	6 RMB
Step 3	tris(4-bromophenyl)methane		1.04 g	
	bis(pinacolato)diboron	25 g/85 RMB	2.47 g	8.40 RMB
	$Pd(dppf)Cl_2$	5 g/400 RMB	275 mg	22 RMB
	potassium acetate	100 g/65 RMB	1.46 g	0.95 RMB
	1,4-dioxane	500 mL/36 RMB	26 mL	1.88 RMB
	CH_2Cl_2	500 mL/8.8 RMB	800 mL	14.08 RMB
	Na_2SO_4	500 g/10 RMB	2 g	0.04 RMB
	petroleum ether	500 mL/7.3 RMB	200 mL	2.92 RMB
	silica gel	500 g/15 RMB	200 g	6 RMB
Step 4	tridecan-7-one	25 g/891 RMB	5.48 g	195.31RMB
	ethanol	500 mL/7 RMB	85 mL	1.19 RMB
	pyridine	500 mL/85 RMB	42 mL	7.14 RMB
	hydroxylamine hydrochloride	100 g/45 RMB	4 g	1.8 RMB
	HCl	500 mL/15 RMB	20 mL	0.6 RMB
	petroleum ether	500 mL/7.3 RMB	600 mL	8.76 RMB
	Na_2SO_4	500 g/10 RMB	6 g	0.12 RMB
Step 5	tridecan-7-one oxime		5.85 g	
	toluene	500 mL/12 RMB	112 mL	2.69 RMB
	Red Al (70% in toluene)	100 g/108 RMB	36.3 g	39.2 RMB
	HCl	500 mL/15 RMB	32 mL	0.96 RMB
	petroleum ether	500 mL/7.3 RMB	900 mL	13.14 RMB
	NaOH	500 g/55 RMB	40 g	4.4 RMB
	Na_2SO_4	500 g/10 RMB	2 g	0.04 RMB
Step 6	tridecan-7-amine		5.29 g	
	perylene-3,4,9,10-tetracarboxylic dianhydride (90% purity)	25 g/109 RMB	4.16 g	18.14 RMB
	anhydrous zinc acetate	100 g/59 RMB	1.41 g	0.84 RMB
	imidazole	25 g/40 RMB	21 g	33.6 RMB

	methanol	500 mL/6.5 RMB	30mL	0.39 RMB
Step 7	PDI		6.48 g	
	bromine	500 g/85 RMB	124 g	21.08 RMB
	CH_2Cl_2	500 mL/8.8 RMB	810 mL	14.26 RMB
	sodium sulfite	500 g/47 RMB	50 g	4.7 RMB
	petroleum ether	500 mL/7.3 RMB	1500mL	21.9 RMB
	Na_2SO_4	500 g/10 RMB	2 g	0.04 RMB
	silica gel	500 g/15 RMB	300 g	9 RMB
Step 8	PDI-Br (60% yield)		4.29 g	
	TPM-Pin_3		0.8 g	
	$Pd(PPh_3)_4$	5 g/280 RMB	0.8 g	44.8 RMB
	K_2CO_3	500 g/89 RMB	50.2 g	8.94 RMB
	tricaprylylmethylammonium chloride	25mL/65RMB	5 mL	13 RMB
	toluene	500 mL/12 RMB	400 mL	9.6 RMB
	CH_2Cl_2	500 mL/8.8 RMB	1000mL	17.6 RMB
	petroleum ether	500 mL/7.3 RMB	250mL	3.65 RMB
	Na_2SO_4	500 g/10 RMB	2 g	0.04 RMB
	silica gel	500 g/15 RMB	250 g	7.5 RMB
Total cost	**PM-PDI_3**			**620.01 RMB**

8. Synthesis and Characterization

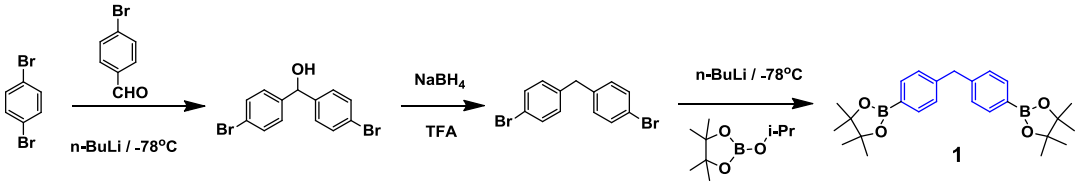

Scheme S1. Synthetic routes of compound 1.

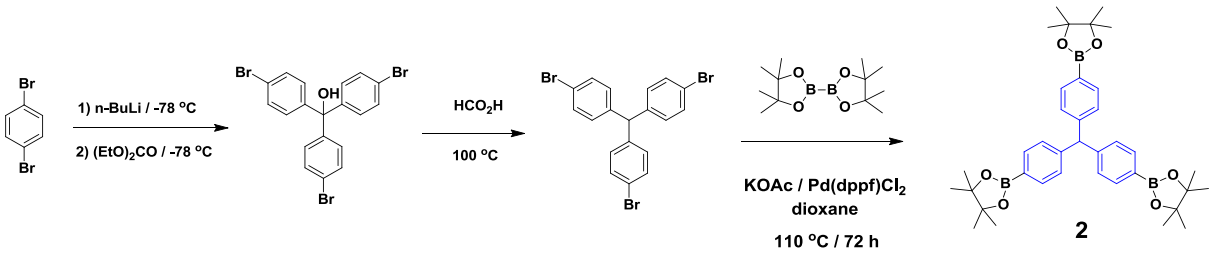

Scheme S2. Synthetic routes of compound 2.

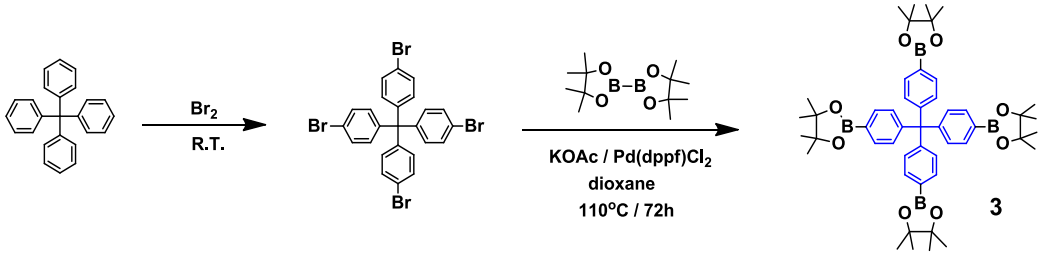

Scheme S3. Synthetic routes of compound 3.

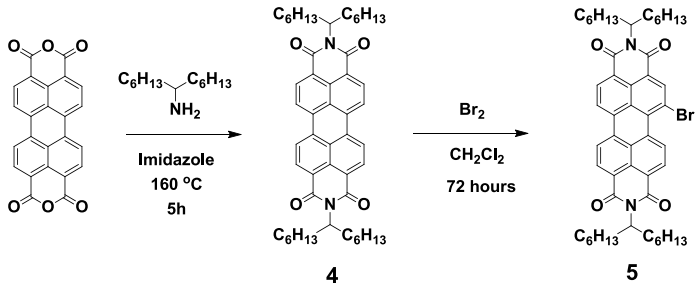

Scheme S4. Synthetic routes of compound 5.

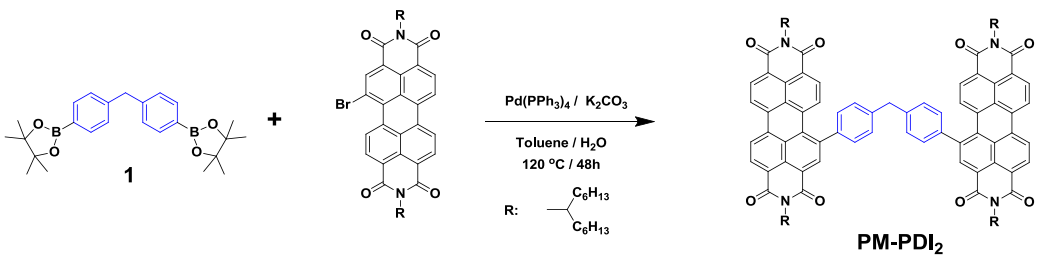

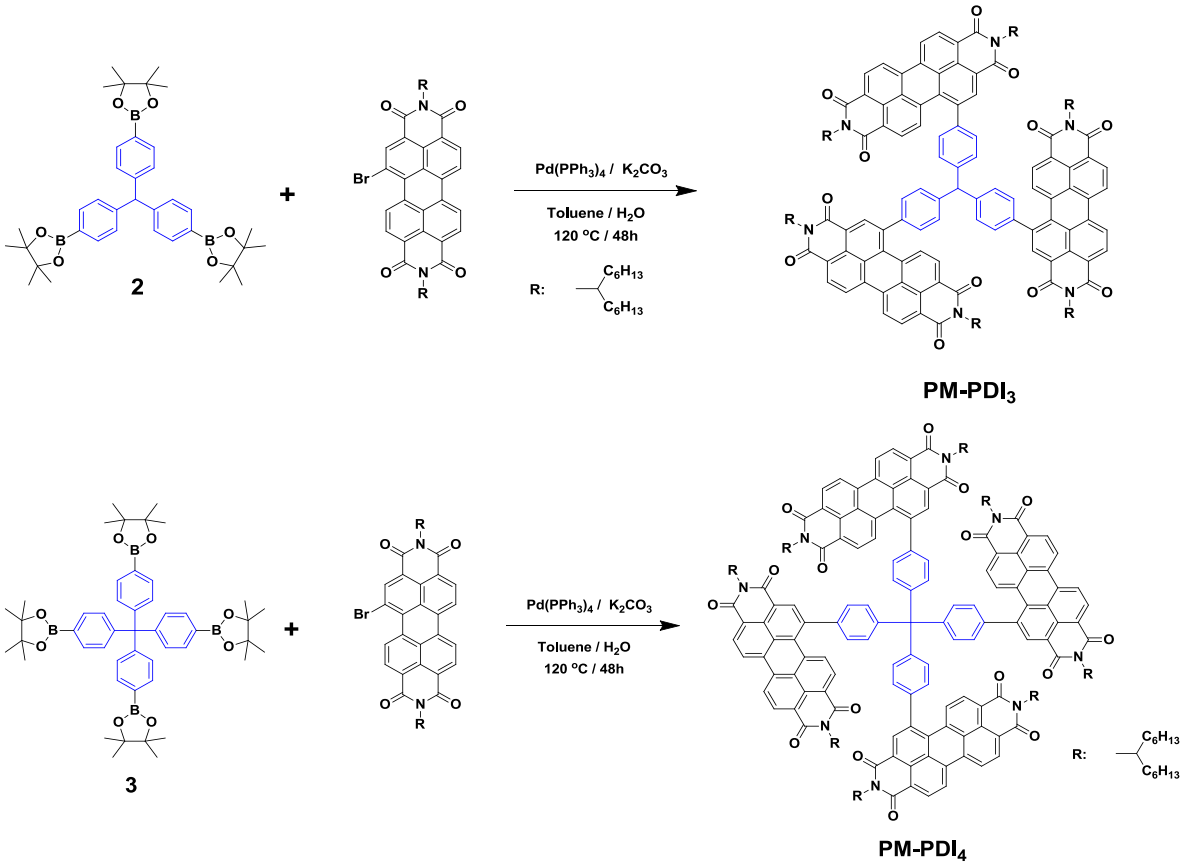

Scheme S5. Synthetic routes of three target molecules.

The details of synthesis

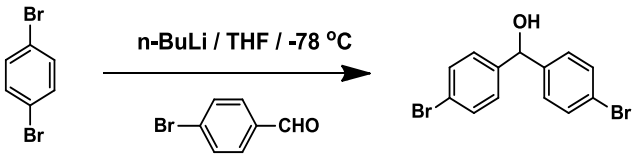

Bis(4-bromophenyl)methanol. To a solution of 1,4-dibromobenzene (5.66 g, 24.0 mmol) in THF (45 mL) at -78 ℃ was added *n*-BuLi (8.8 mL, 22.0 mmol, 2.5 M in hexane) dropwise. The slurry was stirred for 1h and added to a solution of 4-bromobenzylaldehyde (3.7 g, 20 mmol) in THF (50 mL) which was cooled at -78 ℃. The yellow solution was allowed to warmed to room temperature and stirred for 2 h before pouring into water. The mixture was extracted with ethyl acetate. The combined organic fractions were washed with water and dried over Na_2SO_4. The crude product was purified by silicon chromatography (petroleum ether / CH_2Cl_2, 1:2,

V/V) to get pure product as a white solid (5.51 g, 81% yield). ^{1}H NMR (400 MHz, *CDCl$_3$*) δ 7.45 (d, J = 8.5 Hz, 4 H), 7.21 (d, J = 8.3 Hz, 4 H), 5.74 (d, J = 3.3 Hz, 1 H), 2.21 (d, J = 3.4 Hz, 1 H).

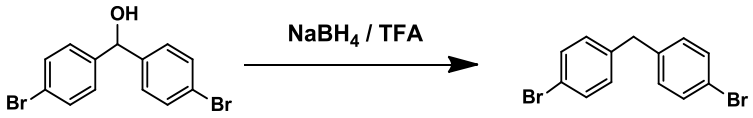

Bis(4-bromophenyl)methane. To a solution of bis(4-bromophenyl)methanol (2.91 g, 8.5 mmol) in TFA (95 mL) was added sodium borohydride (3.22 g, 85.1 mmol) in small portions at room temperature over 10 min. The resulting white slurry was stirred for 1h before pouring into water. The suspension was carefully made alkaline with aqueous sodium hydroxide solution. The mixture was extracted with CH_2Cl_2. The combined organic fraction was washed with water, brine and dried over Na_2SO_4. Removal of solvents followed by filtering through a short silica gel column (hexane) afforded desired product as a white solid (2.07 g, 75%). ^{1}H NMR (300 MHz, *CDCl$_3$*) δ 7.39 (d, 4 H), 7.01 (d, 4 H), 3.86 (s, 2 H).

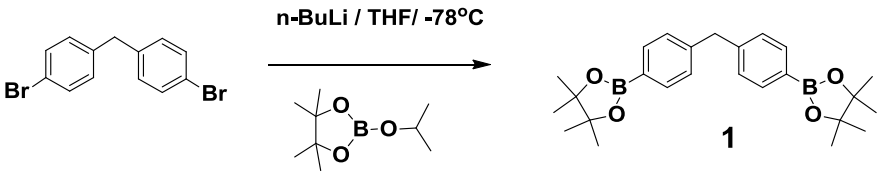

bis(4'-(3,3,4,4-tetramethyl-2,5,1-dioxaboryl)phenyl)methane (1). Bis(4-bromophenyl)methane (1.67 g, 5.12 mmol, 1 eq) was dissolved in 80 mL THF and cooled to -78 ℃. Then *n*-BuLi (2.5 M, 5.0 mL, 12.5 mmol, 2.4 eq) was syringed into the cooled solution over the course of 3 min. Then neat isopropyl pinacol borate (4.5 mL, 21.6 mmol, 4.2 eq) was quickly added in stream. The mixture was stirred at -78 ℃ for 15 min and allowed to warm to room temperature slowly. After 3 hours, the reaction was carefully quenched with water (100 mL). The mixture was extracted with dichloromethane (3×100 mL) and combined the organic layers were washed with

brine and dried over Na_2SO_4. After concentrating under reduced pressure, the crude product was purified by silicon chromatography (petroleum ether / CH_2Cl_2, 1:2, V/V) to get pure product as white powder (946 mg, 44% yield). ^{1}H NMR (400 MHz, *$CDCl_3$*, ppm): δ 7.73 (d, 4H), 7.18 (d, 4H), 4.00 (s, 2H), 1.32 (s, 24H).

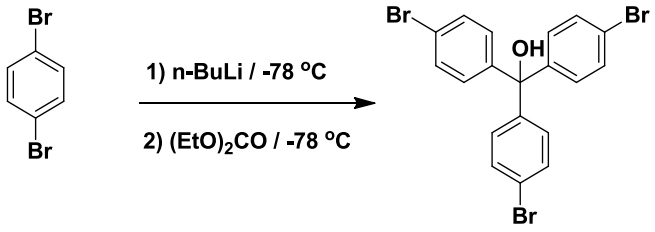

Tris(4-bromophenyl)methanol. p-dibromobenzene (8.7 g, 37.2 mmol) and THF (135 mL) were added to a flame-dried 3-neck 300 mL round-bottom flask equipped with a stirbar, three-way vacuum inlet adapter, glass stopper, and septum. The solution was cooled to -78 ℃ and n-BuLi (2.5 M in hexanes, 13.5 mL, 33.8 mmol) was added dropwise. Separately, diethyl carbonate (1.02 mL, 8.5 mmol) was dissolved in THF (3 mL) in a flame-dried 300 mL round-bottom flask equipped with a stirbar, septum, and nitrogen inlet needle and cooled to -78 ℃. After 3 h, the solution containing the lithiated species was transferred to the diethyl carbonate solution through a cannula and the solution was subsequently allowed to warm to R.T. After 6 h, the reaction mixture was quenched with saturated aqueous NH_4Cl (50 mL). The crude product was extracted with EtOAc. The organic fractions were collected, washed with brine, and dried over anhydrous $MgSO_4$. The crude solid was dry loaded onto SiO_2 and chromatographed using a gradient of hexanes to 25% EtOAc:hexanes (v/v) to yield 3.38 g (80%) product as a white solid. ^{1}H NMR (400 MHz, *$CDCl_3$*, ppm): δ 7.45 (6H), 7.12 (6H), 2.70 (1H).

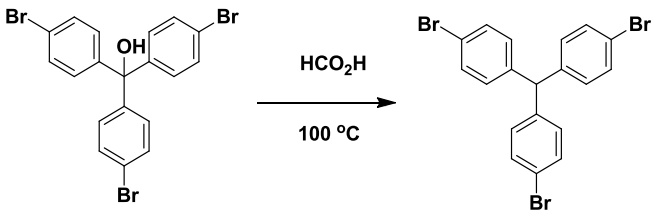

Tris(4-bromophenyl)methane. Tris(4-bromophenyl)methanol (1.25 g, 2.52 mmol) was added to a 50 mL round-bottom flask. Formic acid (95% in H_2O, 25 mL) was added slowly. A condenser was then attached to the flask and the bright yellow suspension was heated to 100 ℃ for 19 h to give a dull yellow suspension. The remaining acid was neutralized with saturated aqueous Na_2CO_3 (100 mL), which caused a white solid to precipitate. The aqueous suspension was washed with Et_2O (3 x 40 mL) and the combined organic phases were washed with brine, dried with $MgSO_4$ and evaporated. The resulting crude solid was run through a plug of SiO_2 in pentane, enabling the isolation of product (0.897 g, 74% yield) as a white crystalline solid. ^{1}H NMR (400 MHz, *CDCl*$_3$, ppm): δ 7.42 (6H), 6.93 (6H), 5.40 (1H).

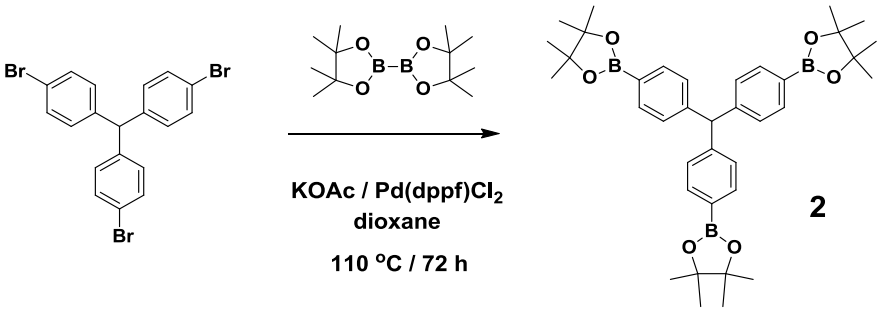

Tris(4-(4,4,5,5-tetramethyl-1,3,2-dioxaborolan-2-yl)phenyl)methane (2)

In a dried 500 mL three-neck round bottle flask was added anhydrous dioxane (20 mL) and KOAc (0.836 g, 8.8 mmol), then bubbled with Ar_2 for 30 minutes. Tris(4-bromophenyl)methane (4.23 g, 8.8 mmol), bis(pinacolato)diboron (0.92 g, 3.52 mmol) and Pd(dppf)Cl_2 (150 mg, 0.205 mmol) were added respectively under Ar_2 protection. The mixture was heated to 110 ℃ for 72 h and was monitored using TLC. Then the reaction mixture was cooled to room temperature, removed the dioxane under reduced pressure and poured into water. The solution was stirred for 10 minutes

and filtered, washed the residue by water and dried under vacuum. The residue was dissolved in dichloromethane and purified using flash column chromatograph with petroleum ether / CH_2Cl_2, (1:1, V/V) as eluent to remove the impurities, then CH_2Cl_2 as eluent to obtain the product as a white product (3.17 g, 58% yield). ^{1}H NMR (400 MHz, *CDCl*$_3$, ppm): δ 7.71 (d,6H), 7.10 (d,6H),5.57 (s, 1H), 1.33 (s, 36H). ^{13}C NMR (100 MHz, *CDCl*$_3$, ppm) δ 146.63, 134.82, 128.92, 83.70, 76.69, 57.30, 24.84. HRMS: $C_{37}H_{49}B_3NaO_6$ (M^+ + Na), calcd, 645.3706; found, 645.3664.

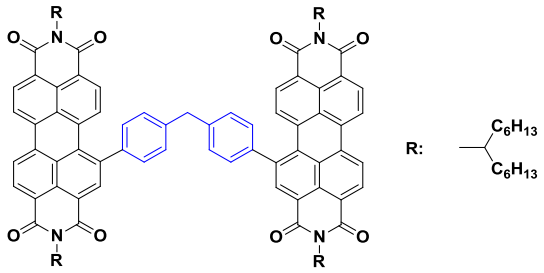

Synthesis of **PM-PDI$_2$**. A three-neck flask charged with compound **1** (60 mg, 0.143 mmol), PDI-Br (300 mg, 0.36 mmol), $Pd(PPh_3)_4$ (80 mg, 0.069 mmol), K_2CO_3 (2.9 g, 21 mmol) , Tricaprylylmethylammonium chloride (2 drops) and degassed in dry toluene / H_2O (21 mL / 10.5 mL). The reaction mixture was heated at 120 ℃ for 48 h. After cooled to room temperature, the reaction mixture was extracted by CH_2Cl_2. The crude product was purified by silicon chromatography (petroleum ether / CH_2Cl_2, 1:2, V/V) to get pure product as a red solid (180 mg, 75% yield). ^{1}H NMR (400 MHz, $CDCl_3$): δ 8.71-8.59 (m, 10H), 8.20-8.13 (m, 2H), 7.97 (d, 4H), 7.51 (d, 2H), 7.41 (d, 4H), 5.23-5.16 (m, 4H), 4.26 (s, 2H), 2.24-2.19 (m, 8H), 1.84-1.81 (m, 8H), 1.28-1.20 (m, 68H), 0.83-0.79 (m, 24H). ^{13}C NMR (400 MHz, $CDCl_3$): δ 164.80, 164.63, 163.72, 163.54, 141.54, 141.12, 140.70, 136.66, 135.96, 134.78, 134.48, 132.44, 131.59, 131.32, 130.99, 130.81, 130.58, 129.92, 129.16, 128.81, 128.50, 128.05, 127.55, 123.66, 123.50, 123.02, 122.80, 122.64, 122.07, 54.71, 54.62, 41.31, 32.33, 31.75, 31.72, 29.22, 29.19, 26.87, 22.58, 22.57, 14.05, 14.04. FT-IR (KBr): 2954, 2922, 2853, 1698, 1657, 1591, 1505, 1455,1407, 1364, 1331, 1245, 1173, 810, 748. HRMS: $C_{113}H_{133}N_4O_8$ (M^+ +H), calcd, 1675.0157; found.1675.0172.

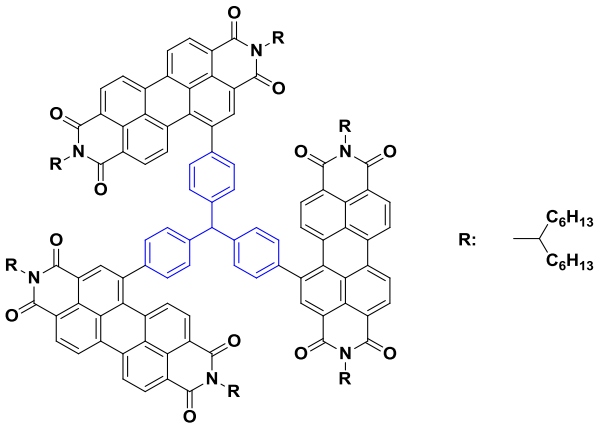

Synthesis of **PM-PDI$_3$**. A three-neck flask charged with compound **2** (100 mg, 0.161 mmol, 1.0 eq), PDI-Br (536 mg, 0.643 mmol, 4.0 eq), $Pd(PPh_3)_4$ (100 mg, 0.087 mmol), K_2CO_3 (6.27 g, 0.045mol) , tricaprylylmethyl- ammonium chloride (2 drops) and degassed in dry toluene / H_2O (50 mL / 25 mL). The reaction mixture was heated at 120 ℃ for 48 h. After cooled to room temperature, the reaction mixture was extracted by CH_2Cl_2. The crude product was purified by silicon chromatography (petroleum ether /CH_2Cl_2,1:3, V/V) to get pure product as a dark red solid (125 mg, 31% yield). ^{1}H NMR (400 MHz, $CDCl_3$): δ 8.65 (m, 10H), 8.15-8.05 (m, 4H), 7.60-7.47 (m, 8H), 5.34-5.09 (m, 6H), 2.25-2.14 (m, 8H), 1.83 (m, 8H), 1.26-1.15 (m, 68H), 0.78 (d, 24H). ^{13}C NMR (400 MHz, $CDCl_3$): δ 164.69, 163.67, 143.64, 141.52, 141.32, 136.63, 134.91, 134.54, 133.95, 133.83, 132.59, 131.42, 130.45, 129.94, 129.75, 129.28, 129.02, 128.66, 128.13, 127.66, 124.47, 123.55, 123.15, 122.72, 56.11, 54.79, 32.40, 32.31, 31.76, 31.68, 29.71, 29.22, 29.13, 26.90, 26.85, 22.58, 22.52, 14.02, 13.98. FT-IR (KBr): 2953, 2925, 2855, 1699, 1657, 1590, 1500, 1454,1404, 1365, 1330, 1242, 1173, 812, 750. HRMS: $C_{169}H_{196}N_6O_{12}$ (M^+), calcd, 2502.4945; found 2502.4975.

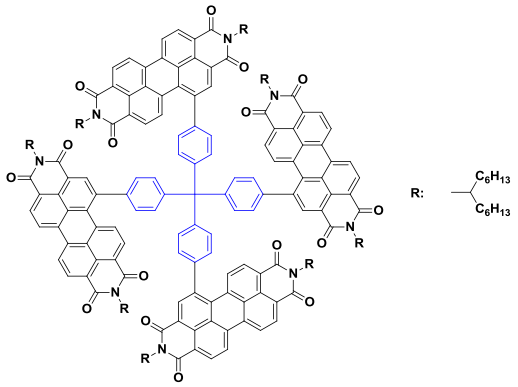

Synthesis of **PM-PDI$_4$**.[3] A three-neck flask charged with tetrakis(4-(4,4,5,5-tetramethyl-1,3,2-dioxaborolan-2-yl)phenyl)methane[3] (66 mg, 0.080 mmol, 1.0 eq), PDI-Br[4] (333.6 mg, 0.405 mmol, 5 eq), $Pd(PPh_3)_4$ (40 mg, 0.035 mmol), K_2CO_3 (165.6 mg, 1.2 mmol) and degassed dry THF / H_2O (12 mL / 6 mL). The reaction mixture was heated at 80 ℃ for 72 h. After cooled to room temperature, the reaction mixture was extracted by CH_2Cl_2. The crude product was purified by silicon chromatography (petroleum ether / CH_2Cl_2, 1:3, V/V) to get pure product as a dark red solid (72 mg, 27% yield). ^{1}H NMR (400 MHz, $CDCl_3$): δ 8.73-8.63 (m, 5H), 8.05 (m, 2H), 7.69-7.60 (m, 4H), 5.19 (m, 2H), 2.24-1.84 (m, 8H), 1.30-0.88 (m, 34H), 0.81-0.66 (m, 12H). FT-IR (KBr): 2952, 2925, 2855, 1699, 1658, 1590, 1499, 1455, 1407, 1331, 1246, 1174, 812, 750. HRMS: $C_{225}H_{261}N_8O_{16}$ (M^+ +H), calcd, 3332.9923; found, 3332.9910.

9. Spectroscopic data

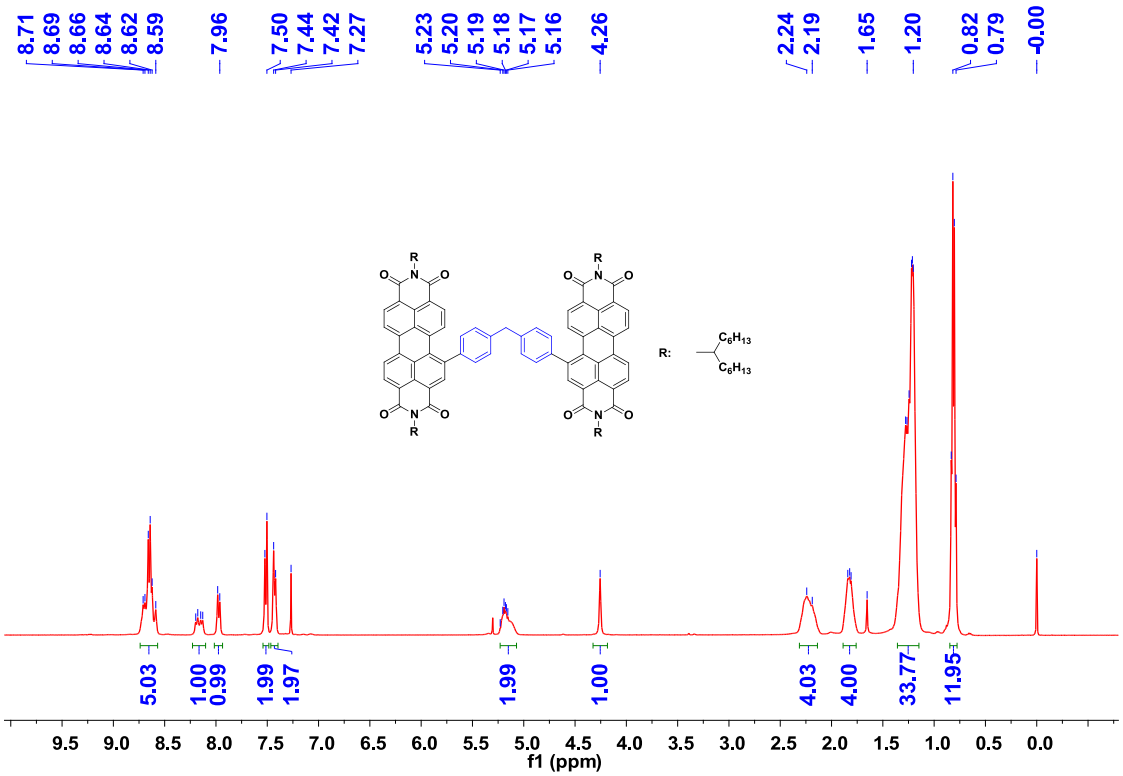

Figure S7. ^{1}H NMR spectrum of compound **PM-PDI$_2$.**

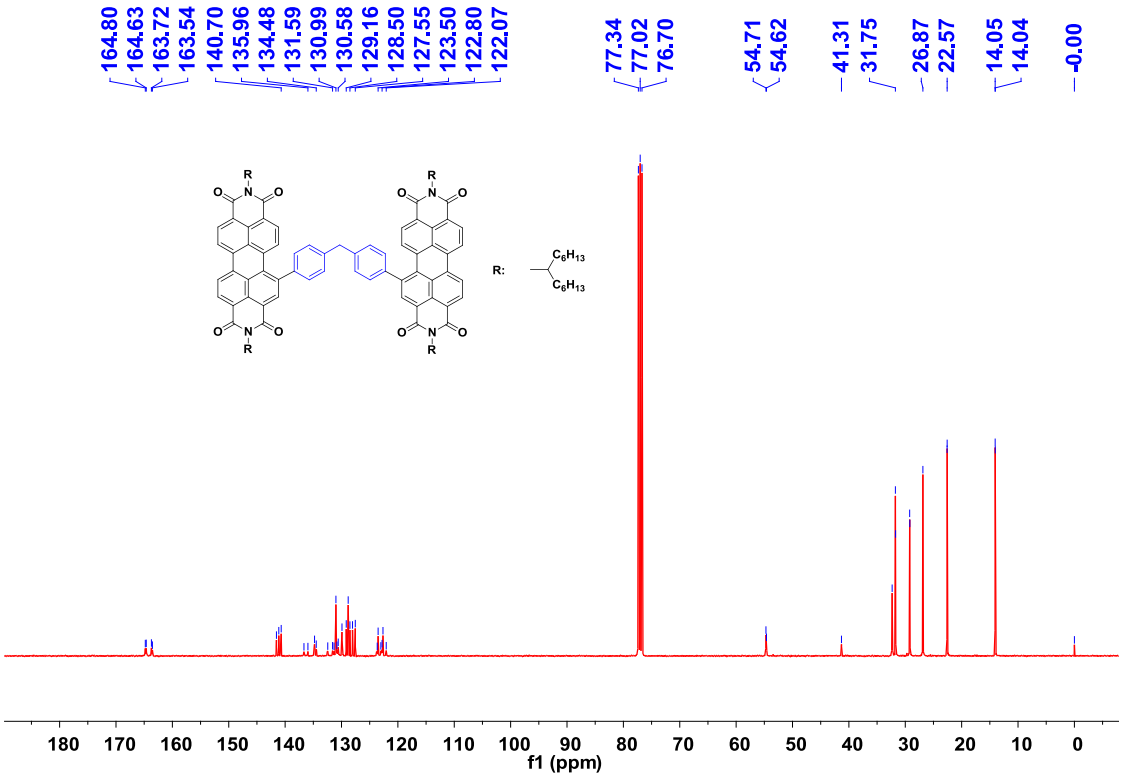

Figure S8. ^{13}C NMR spectrum of compound **PM-PDI$_2$.**

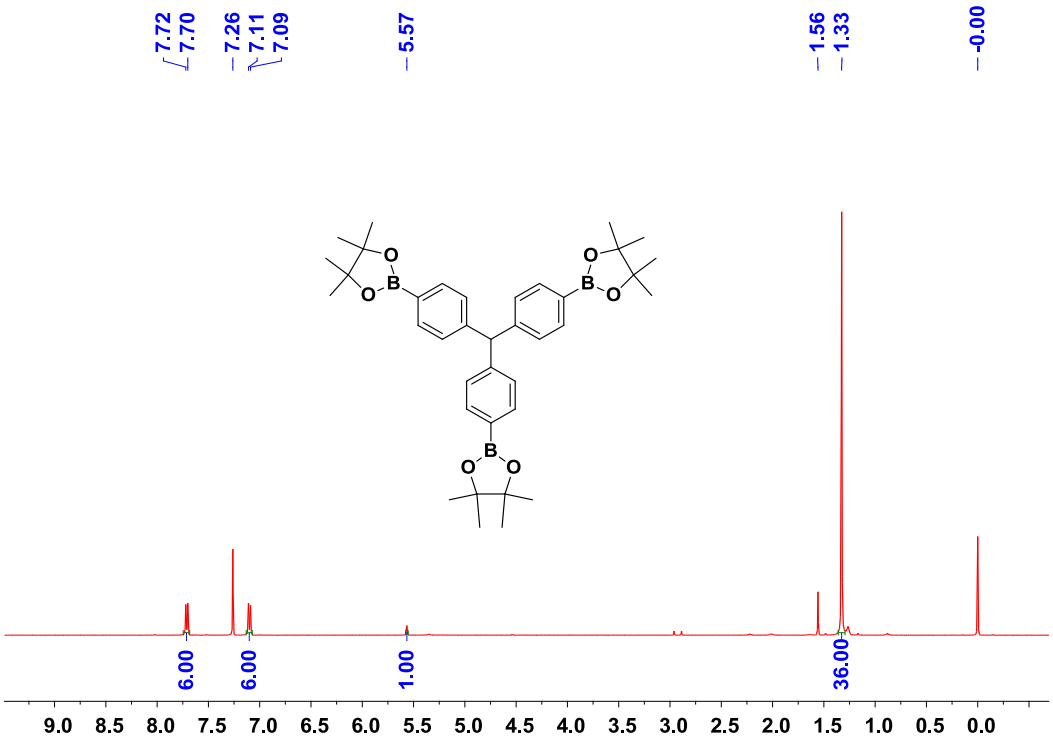

Figure S9. ^{1}H NMR spectrum of compound **2**

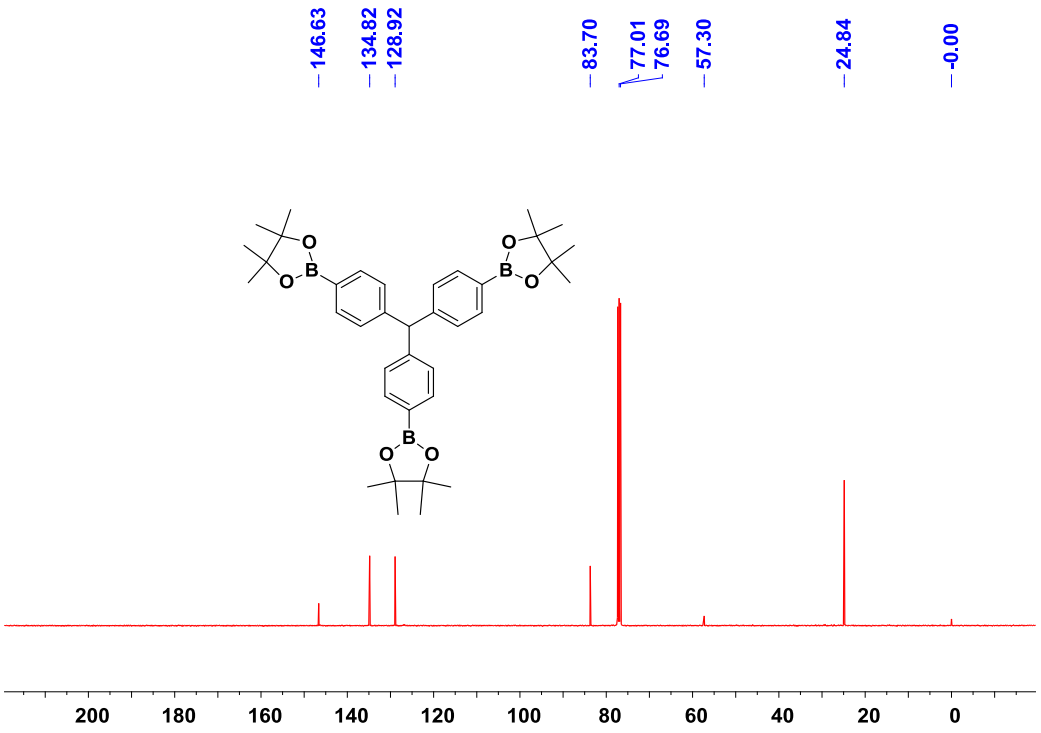

Figure S10. ^{13}C NMR spectrum of compound **2**.

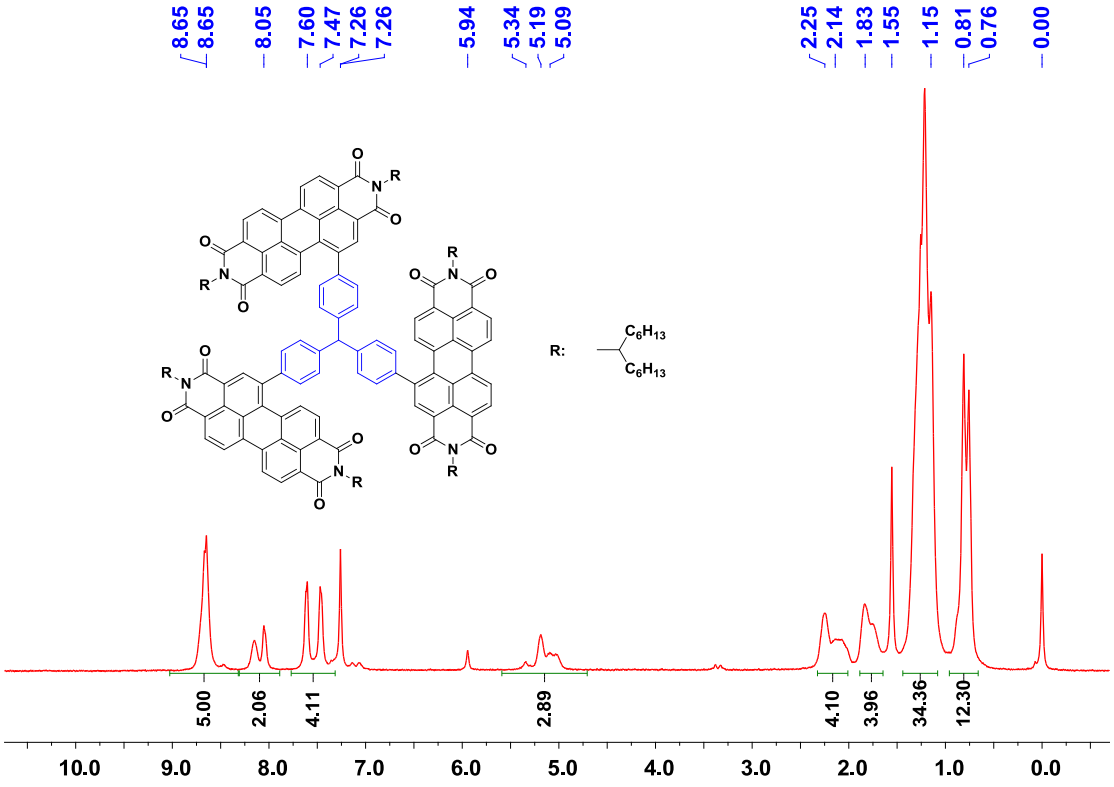

Figure S11. ^{13}C NMR spectrum of compound **PM-PDI$_3$.**

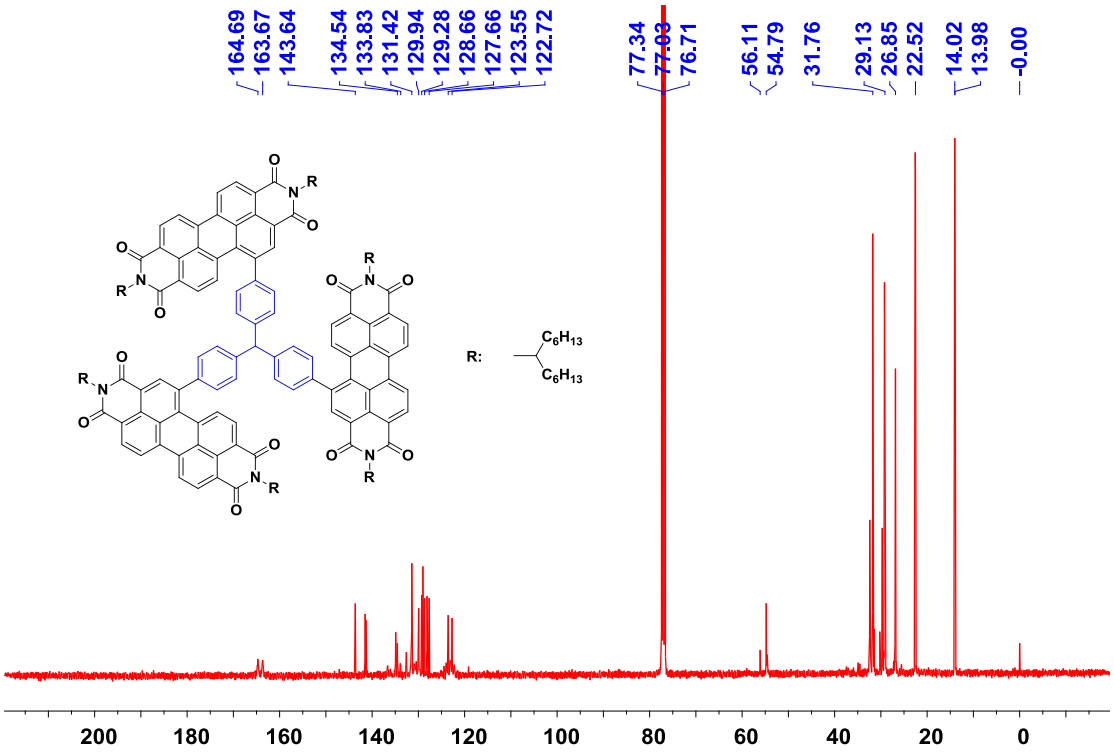

Figure S12. ^{1}H NMR spectrum of compound **PM-PDI$_3$.**

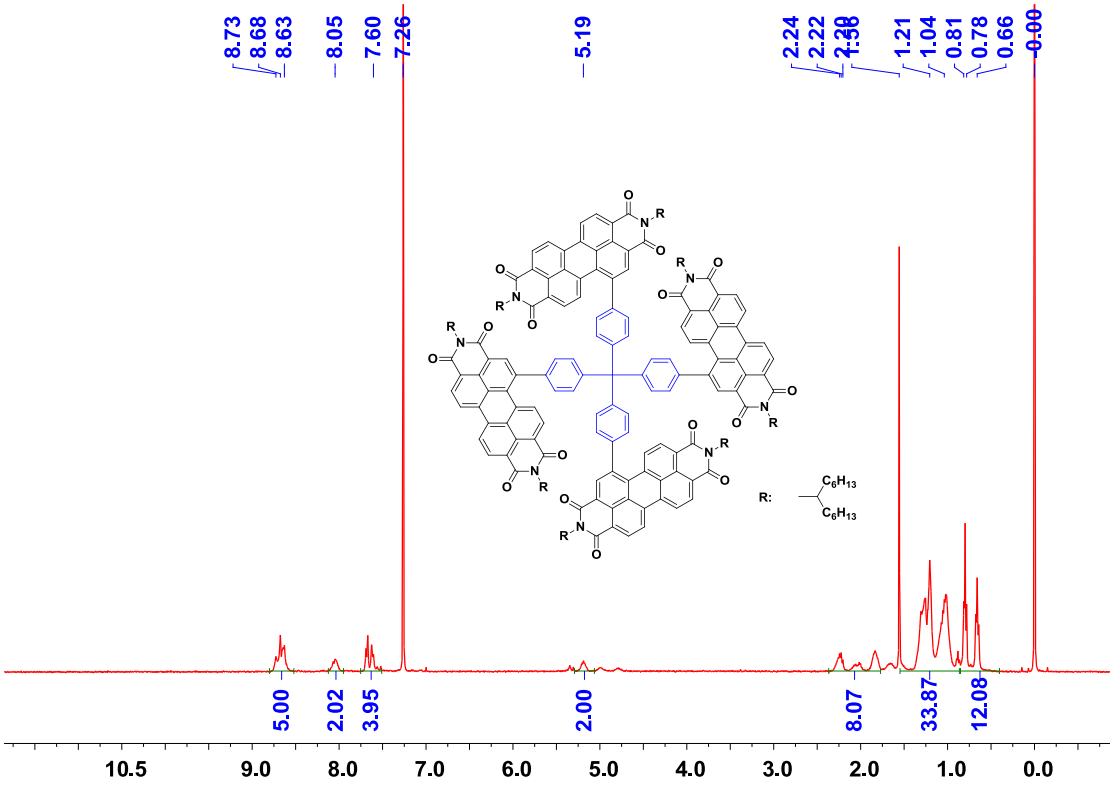

Figure S13. ^{1}H NMR spectrum of compound **PM-PDI$_4$.**

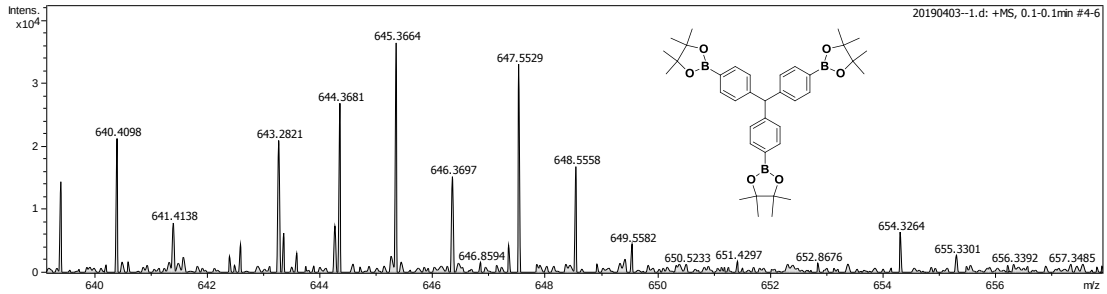

Figure S14. HRMS profile of compound **2.**

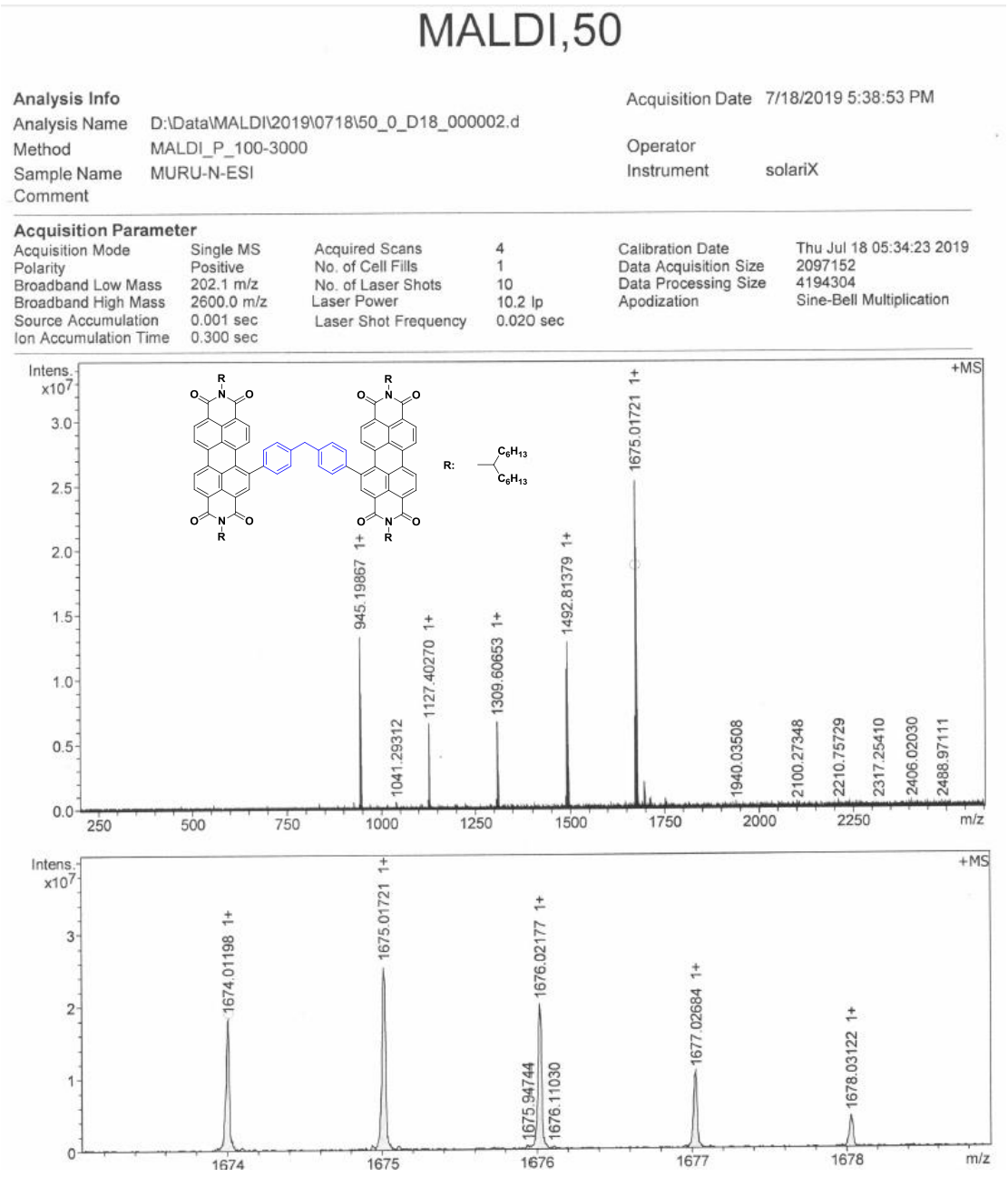

Figure S15. MAIDI-TOF profile of **PM-PDI$_2$.**

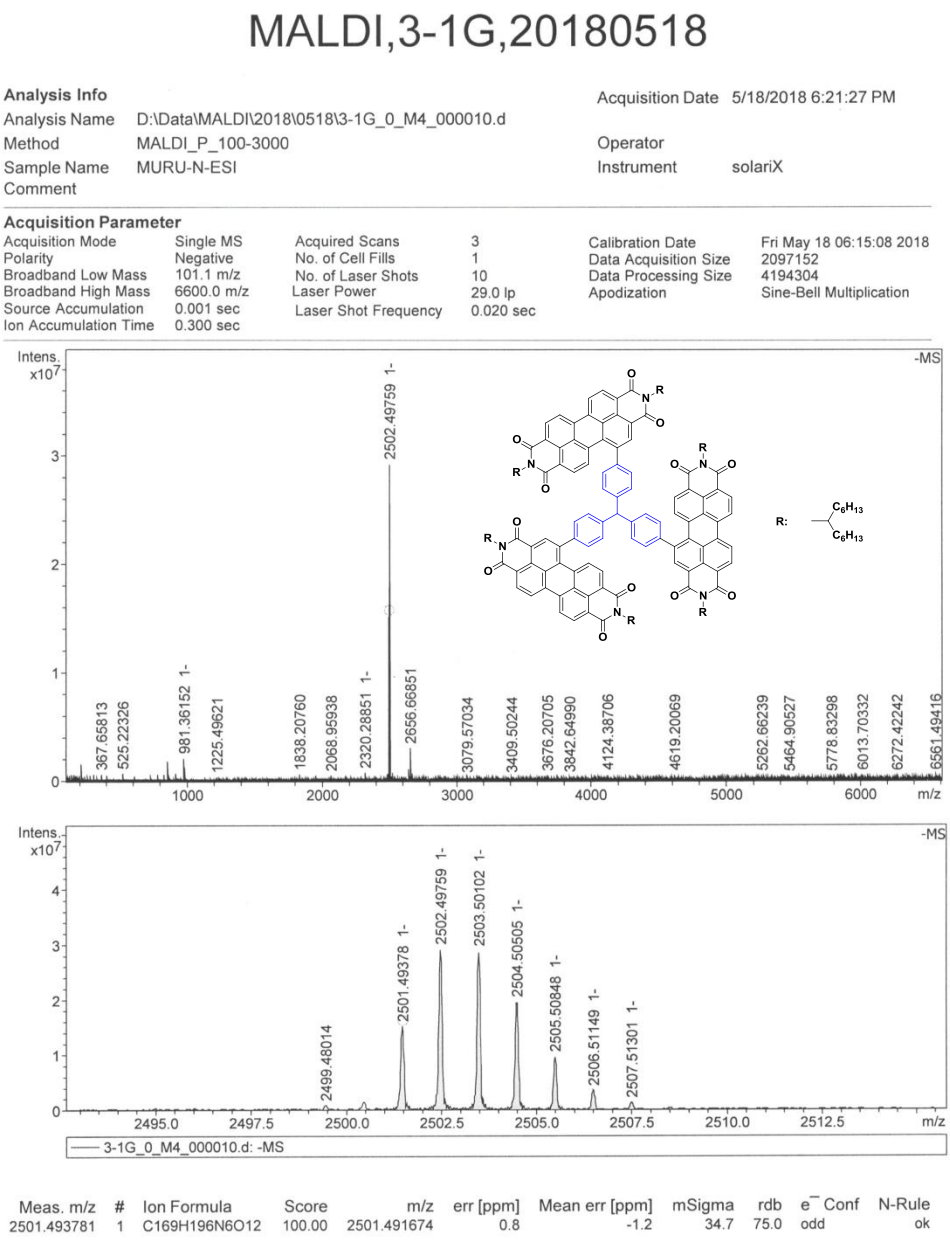

Figure S16. MAIDI-TOF profile of compound **PM-PDI$_3$.**

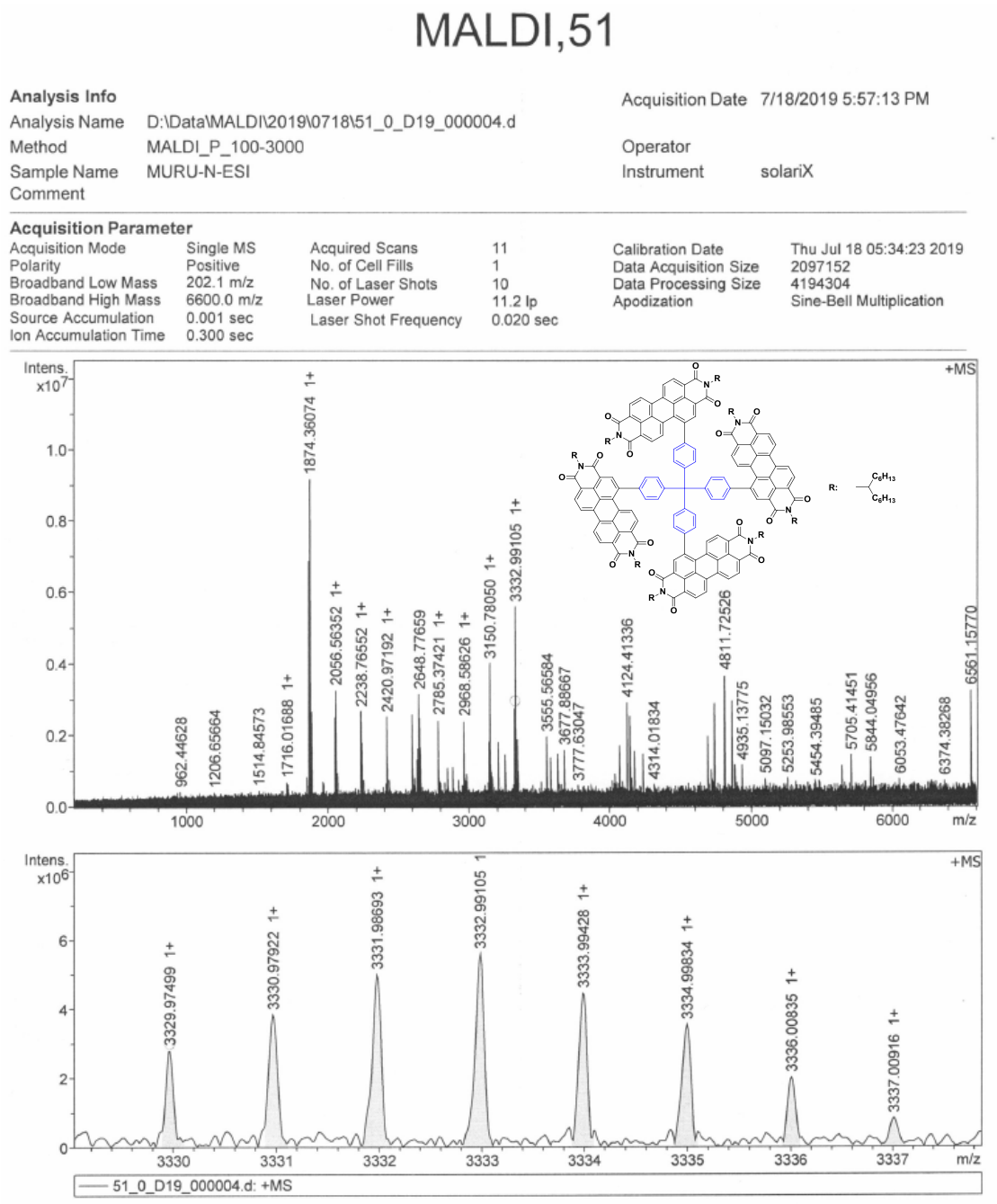

Figure S17. MAIDI-TOF profile of compound **PM-PDI$_4$.**

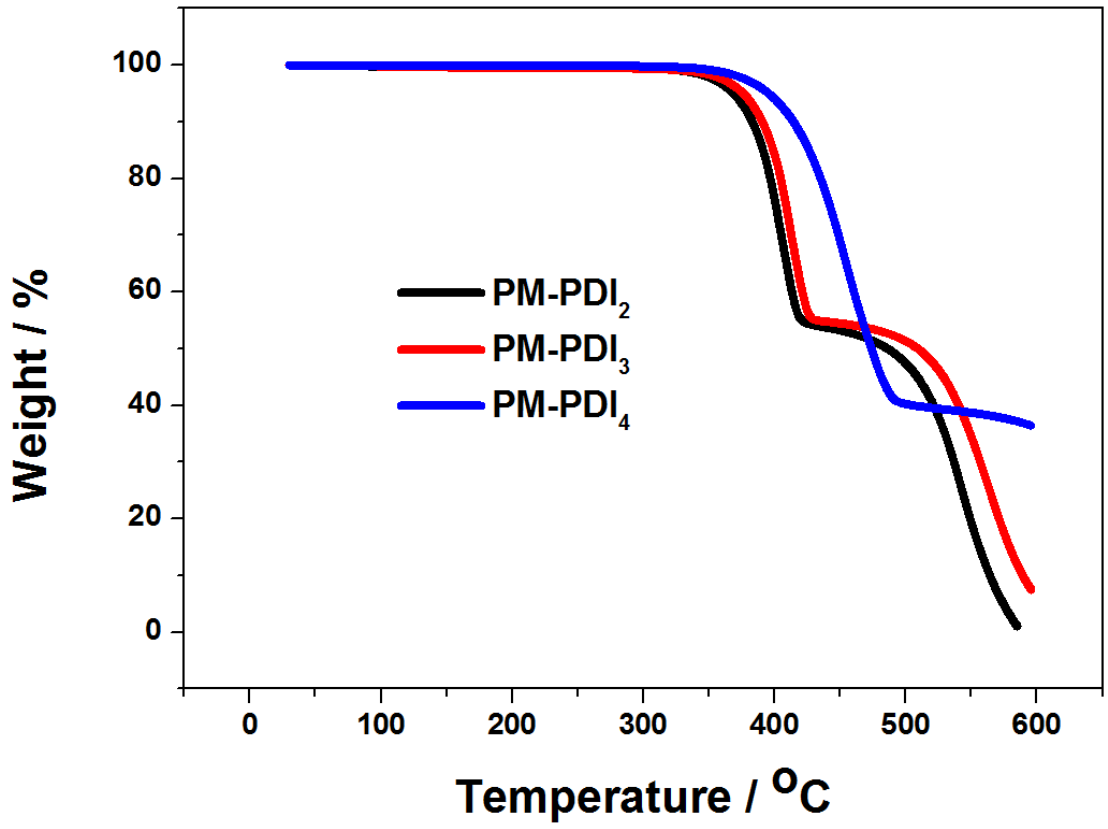

Figure S18. TGA profile of three compounds**.**

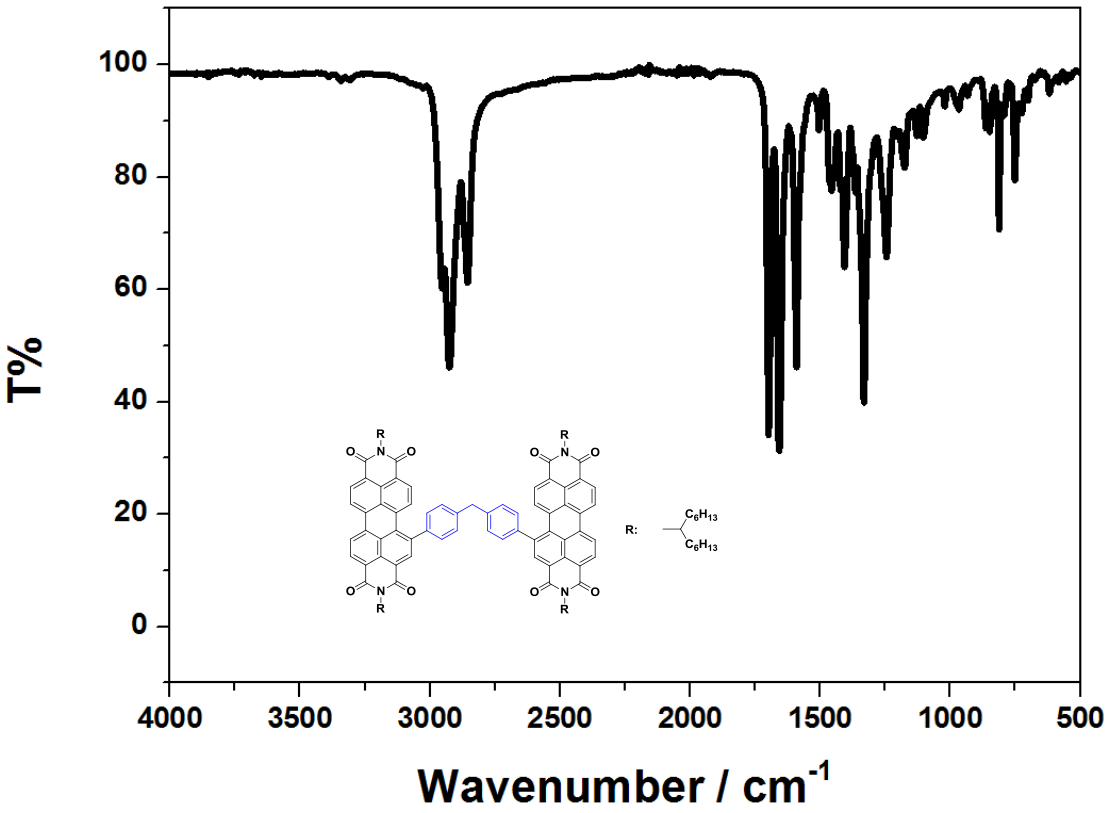

Figure S19. FT-IR spectrum of compound **PM-PDI$_2$.**

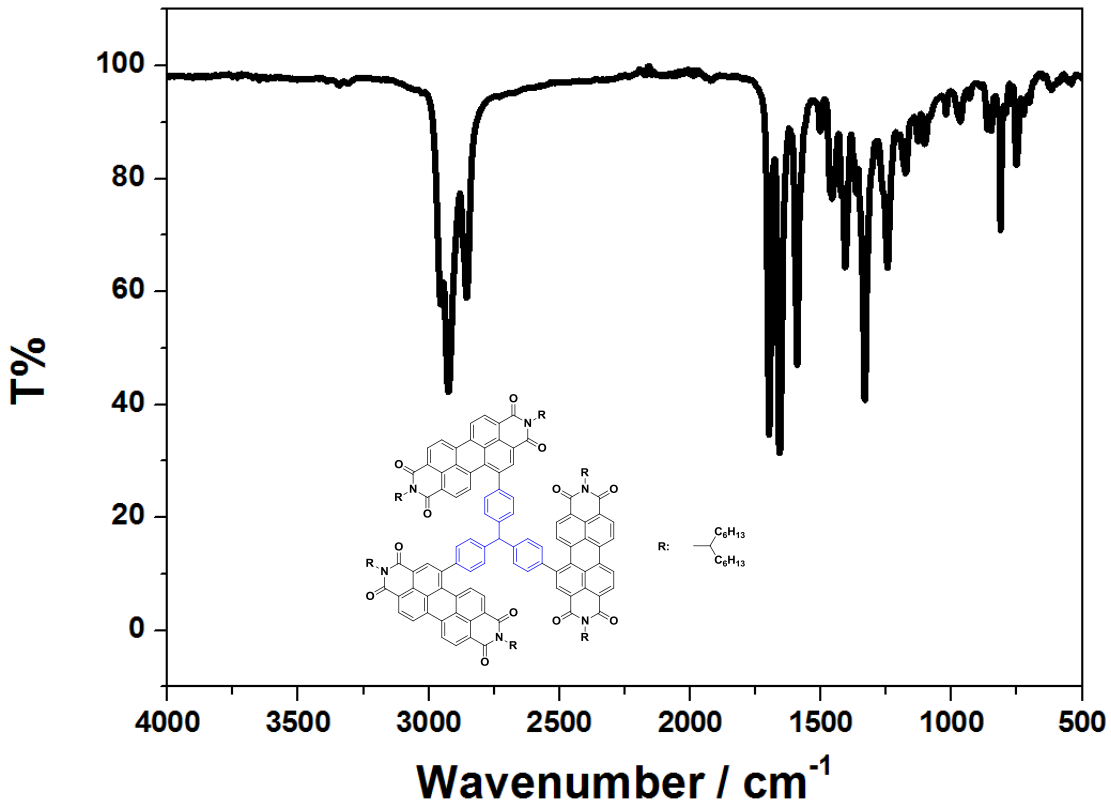

Figure S20. FT-IR spectrum of compound **PM-PDI$_3$.**

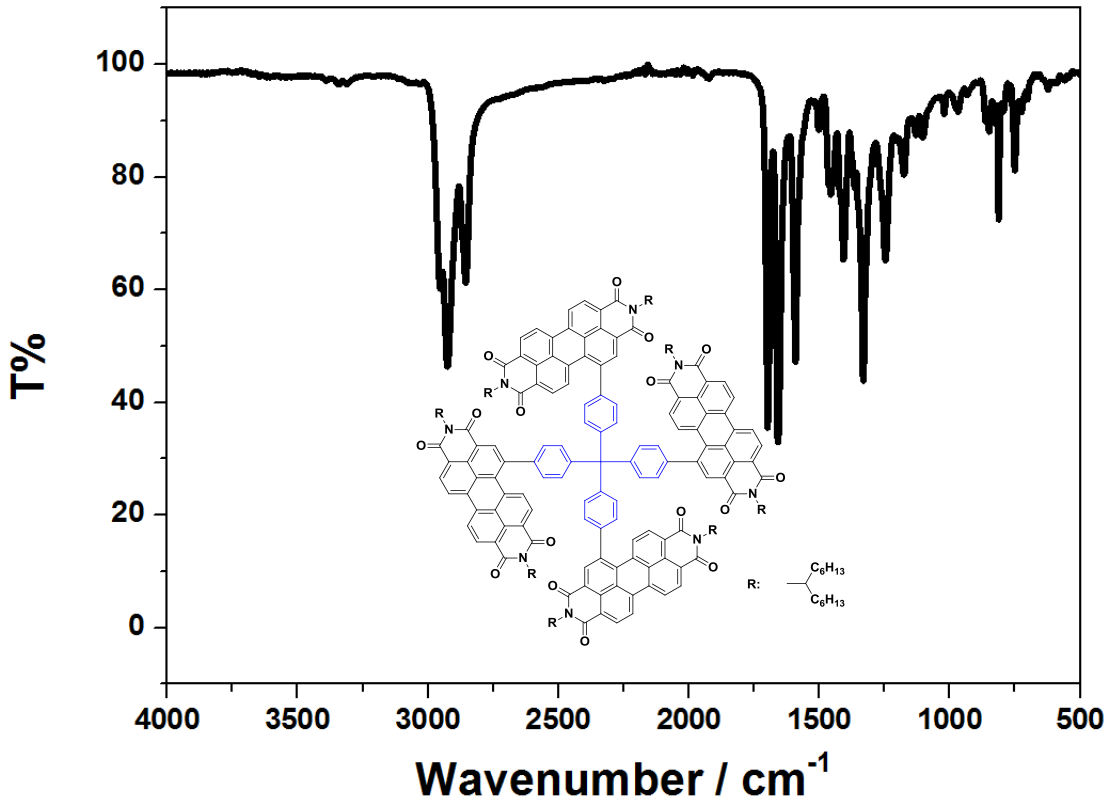

Figure S21. FT-IR spectrum of compound **PM-PDI$_4$.**

10. Reference

1. D. Sun, D. Meng, Y. Cai, B. Fan, Y. Li, W. Jiang, L. Huo, Y. Sun and Z. Wang, *J. Am. Chem. Soc.*, **2015**, 137, 11156.

2. P. Li, T. J. Sisto, E. R. Darzi and R. Jasti, *Org. Lett.*, **2014**, 16, 182.

3. Liu, Y.; Lai, J. Y. L.; Chen, S.; Li, Y.; Jiang, K.; Zhao, J.; Li, Z.; Hu, H.; Ma, T.; Lin, H.; Liu, J.; Zhang, J.; Huang, F.; Yu, D.; Yan, H. *J. Mater. Chem. A.*, **2015**, 3, 13632.

4. Yan, Q.; Zhao, D. *Org. Lett.*, **2009**, 11, 3426.

5. M. J. Frisch, G. W. Trucks, H. B. Schlegel, G. E. Scuseria, M. A. Robb, J. R. Cheeseman, G. Scalmani, V. Barone, G. A. Petersson, H. Nakatsuji, X. Li, M. Caricato, A. Marenich, J. Bloino, B. G. Janesko, R. Gomperts, B. Mennucci, H. P. Hratchian, J. V. Ortiz, A. F. Izmaylov, J. L. Sonnenberg, D. Williams-Young, F. Ding, F. Lipparini, F. Egidi, J. Goings, B. Peng, A. Petrone, T. Henderson, D. Ranasinghe, V. G. Zakrzewski, J. Gao, N. Rega, G. Zheng, W. Liang, M. Hada, M. Ehara, K. Toyota, R. Fukuda, J. Hasegawa, M. Ishida, T. Nakajima, Y. Honda, O. Kitao, H. Nakai, T. Vreven, K. Throssell, J. A. Montgomery, Jr., J. E. Peralta, F. Ogliaro, M. Bearpark, J. J. Heyd, E. Brothers, K. N. Kudin, V. N. Staroverov, T. Keith, R. Kobayashi, J. Normand, K. Raghavachari, A. Rendell, J. C. Burant, S. S. Iyengar, J. Tomasi, M. Cossi, J. M. Millam, M. Klene, C. Adamo, R. Cammi, J. W. Ochterski, R. L. Martin, K. Morokuma, O. Farkas, J. B. Foresman, and D. J. Fox, Gaussian 09, revision A.1; Gaussian, Inc.: Wallingford, CT, 2009.